

Structural and electronic properties of $\text{YBa}_2\text{Cu}_3\text{O}_7$ and $\text{YSr}_2\text{Cu}_3\text{O}_7$ under mechanical and strontium chemical pressures

H. Khosroabadi, B. Mossalla, and M. Akhavan*

Magnet Research Laboratory (MRL), Department of Physics, Sharif University of Technology, P.O. Box 11365-9161, Tehran, Iran

(Received 19 March 2004; revised manuscript received 14 June 2004; published 21 October 2004)

Calculations of structural and electronic properties of two $\text{YBa}_2\text{Cu}_3\text{O}_7$ (YBCO) and $\text{YSr}_2\text{Cu}_3\text{O}_7$ (YSCO) high- T_c cuprate isofamilies for ambient and high mechanical pressures ($-15 \text{ GPa} \leq p_m \leq 15 \text{ GPa}$) have been carried out by pseudopotential density functional theory in the local density approximation employing VASP code. We have analyzed the changes of bond lengths and equilibrium ionic positions due to mechanical pressure on YBCO and YSCO. Negative pressure causes separation of the YBCO unit cell into $\text{Cu}(1)\text{-O}(1)\text{-O}(4)$ and $\text{CuO}_2\text{-Y-CuO}_2$ blocks, similar to the effect of oxygen reduction in YBCO. We have also found that the nonlinear dependence for ionic positions by mechanical pressure, especially for $\text{Cu}(2)$, $\text{O}(4)$, $\text{O}(3)$, and $\text{O}(2)$ ions, causes the redistribution of charge density and the transfer of hole to the CuO_2 planes and CuO chains for both systems. It is concluded that in spite of the larger dT_c/dp_m for YSCO in comparison with YBCO, the charge transfer in YSCO is lower than in YBCO. This apparent discrepancy has been discussed on the basis of the effect of oxygen on dT_c/dp_m and the pressure-induced charge-transfer model. Different structural changes due to mechanical and Sr chemical pressures have been discussed for their opposite effects on T_c . Compressibility and equilibrium unit-cell volume for both systems have also been obtained and compared with experimental and computational reports.

DOI: 10.1103/PhysRevB.70.134509

PACS number(s): 74.72.Bk, 31.15.-p, 81.40.Vw

INTRODUCTION

In recent years, extensive studies have been carried out on high-pressure effects in fullerides,¹ organic superconductors,² and layered high-temperature superconductors (HTSC's).³ These studies have been focused mostly on understanding the superconducting- and normal-state properties of HTSC systems for obtaining the correlation between the two states, explaining the different dT_c/dp_m in different families and compounds, and anisotropic pressure dependence of structural and transport properties. These studies show that the p_m dependence of T_c varies strongly by small changes of the component stoichiometry. For example, $dT_c/dp_m = 0.64 \text{ K/GPa}$,⁴ derived for the $\text{YBa}_2\text{Cu}_3\text{O}_7$ (YBCO) single crystal, is completely different from some isostructural compounds, such as 3 K/GPa (Ref. 5), 5.5 K/GPa (Ref. 6), and 7.4 K/GPa (Ref. 7) for $\text{YSr}_2\text{Cu}_3\text{O}_7$, $\text{YBa}_2\text{Cu}_4\text{O}_8$ (Y124), and the reported superconductor $\text{PrBa}_2\text{Cu}_3\text{O}_{7-\delta}$, respectively. Also, dT_c/dp_m changes from $0\text{--}1$ to $4\text{--}7 \text{ K/GPa}$ for the change of 0.3 oxygen content in the YBCO system.^{3,8} Comparison of the electronic properties of these compounds under pressure gives us a clearer understanding of these differences.

Another advantage of the pressure studies is to obtain a way to reach higher T_c by correct structural or internal parameter changes, for example, by suitable substitution of smaller ions and chemical pressure (p_c).⁹ This idea has been followed by some groups: Licci *et al.*¹⁰ followed this proposal by substitution of Sr at the Ba site in YBCO, and as a result, T_c reduced by 20 K per complete substitution of Sr at the Ba site, Fernandes *et al.*¹¹ have also derived reduction of T_c by complete Gd substitution at the Y site by 2 K . Resistivity and magnetic susceptibility measurements by Lu and Chen¹² have indicated that Sr doping (x) at

the Ba site in the $\text{Y}_2(\text{Ba}_{1-x}\text{Sr}_x)_4\text{Cu}_7\text{O}_{14+\delta}$ phase increases T_c by $7.5 \text{ K}/(\text{Sr formula unit})$, but their samples had a solubility limit between $x=0.1$ and 0.15 . The overall result of these studies indicates that p_c causes a decrease or small increase in T_c , which is in contrast to the result of the mechanical pressure effect with positive dT_c/dp_m . For example, for YBCO, $dT_c/dp_m = 0.64 \text{ K/GPa}$,⁴ while $dT_c/dp_c = (dT_c/dx)(dx/dp_c) = (-20) \times 1/10 = -2.0 \text{ K/GPa}$ (Ref. 10) (dT_c/dp_c is analogous to dT_c/dp_m , with p_c being considered as the effective chemical pressure related to substitution of smaller cation). Also, for Y124, $dT_c/dp_m = +5.5 \text{ K/GPa}$,⁶ and $dT_c/dp_c = (dT_c/dx) \times 1/10 = 1.26 \text{ K/GPa}$ for $0.0 \leq x \leq 0.2$ and -4.33 K/GPa for $0.2 \leq x \leq 0.5$.¹³ As a result, the main question in this regard is the origin of the opposite effects between the chemical and mechanical pressures on T_c for some systems.

To understand this difference, some authors have investigated the similarities and differences between the chemical and mechanical pressure effects on other aspects of these compounds. A Cu nuclear quadrupole resonance experiment in Sr-doped Y124 indicates that both p_m and p_c have the same effect on the direction of spectra shift, but the broadening and shift of peaks are larger in the p_c case.¹⁴ A bond valence sum analysis of neutron diffraction data of the $\text{YBa}_{2-x}\text{Sr}_x\text{Cu}_3\text{O}_{7-\delta}$ system shows that the relaxation of Ba/Sr layer hinders the charge transfer to the CuO_2 planes by p_c ,¹⁰ while p_m causes the charge transfer by the pressure-induced charge transfer (PICT) model. It has also been shown that the only important structural difference between p_c and p_m is the change of separation of $\text{CuO}_2\text{-Y-CuO}_2$ superconducting blocks.¹⁰

To better understand this problem, we need a mechanism that could explain the behavior of dT_c/dp_m . From the experimental point of view, we should differentiate the intrinsic

effects such as charge transfer or bond-length contraction from nonintrinsic effects such as structural phase transition or redistribution of oxygen, which usually are not considered in the electronic structure calculation but can be entered in the experimental results of dT_c/dp_m ,³ and also the cation disorder in substituted samples. To interpret the experimental data, some attempts have been made based on the resonating valence bond,⁹ van Hove singularity,¹⁵ extended Hubbard,¹⁶ and PICT models.¹⁷ The PICT model is presented as redistribution of charge density, and as a result, the increase of hole content in the CuO_2 planes (n_{CuO_2}) in these compounds is considered as a suitable approach to explain dT_c/dp_m . Of course, there are also some reports indicating the insufficiency of this model.^{4,18,19} To compare the experimental data with the models, one needs to determine the electronic parameters such as n_{CuO_2} , $N(E_F)$, the van Hove singularity position, hopping amplitudes, and even vibrational and structural parameters such as phonon frequency distribution, ionic position, bond lengths, and compressibility, in ambient pressure, and their pressure dependences.

Electronic structure calculation based on local density-functional theory (LDFT) is a suitable approach to determine these parameters, excluding the experimental nonintrinsic effects. Although, the application of the LDFT approach in HTSC systems with strongly correlated electrons and antiferromagnetic long-range order in parent compounds is controversial, at least in some aspects of the electronic and structural properties such as optical,²⁰ vibrational,²¹ structural and ionic relaxation,²² Fermi surface,²³ and pressure-induced effects,²⁴ it has been shown to be acceptable. Determination of equilibrium ionic positions in high pressures can help to determine the change of n_{CuO_2} by the bond valence sum technique, which is too hard in experimental studies and they are rare in the literature. In addition, obtaining the equilibrium ionic positions, bond lengths, and their effects on the redistribution of charge density under p_m and p_c is essential for any improved model to describe their correlation. The relation between hole content and ionic positions also helps us to refine the structure for optimization of the superconducting properties, and to get higher T_c .

In this paper, we compare high-pressure effects on two isofamilies of HTSC's: YBCO and its chemical pressured YSCO, both at a stoichiometric oxygen content of 7 by LDFT in the range of $-15 \text{ GPa} \leq p_m \leq 15 \text{ GPa}$ to clarify the electronic and structural properties under mechanical and chemical pressures.

COMPUTATIONAL DETAILS

The total energy calculations have been performed using the *ab initio* pseudopotential in the LDFT. We have used the Vienna *ab initio* simulation package (VASP) code,²⁵ based on the LDFT by using the projector augmented plane-wave method. The lattice parameters in ambient pressure for YBCO taken from experimental studies are $a=3.83 \text{ \AA}$, $b=3.88 \text{ \AA}$, and $c=11.68 \text{ \AA}$. The lattice parameters at ambient pressure for the YSCO tetragonal system have been taken from the experimental data⁵ and then have been changed to orthorhombic symmetry by orthorhombicity factor $100(a$

$-b)/[(a+b)/2]=1.32$, to become $a=3.77 \text{ \AA}$, $b=3.82 \text{ \AA}$, and $c=11.38 \text{ \AA}$, to be compared with the YBCO system. This is a reasonable assumption, because they are very close to the extrapolation of a and b parameters of the Rietveld refinement of the chemically doped $\text{Y}(\text{Ba}_{1-x}\text{Sr}_x)_2\text{Cu}_3\text{O}_{7-\delta}$,¹⁰ though this may make the results for YSCO more qualitative by noting the effect of extra oxygen in these compounds (to be discussed later). The change of lattice parameters by pressure for YBCO, i.e., $\Delta a/\Delta p_m=5.36 \times 10^{-3} \text{ \AA/GPa}$, $\Delta b/\Delta p_m=5.044 \times 10^{-3} \text{ \AA/GPa}$, and $\Delta c/\Delta p_m=3.504 \times 10^{-2} \text{ \AA/GPa}$ (Ref. 26) are derived from extrapolation of the experimental lattice parameters by pressure with constraint on the change of volume by pressure, which have been considered for YSCO too.

The atomic pseudopotential for the Y 4d and 5s, Ba 5p and 6s, Sr 5s, Cu 3d and 4s, and O 2s and 2p orbitals have been employed from the VASP library files. The cutoff energy and k -point sampling in the irreducible Brillouin zone are determined to be 800 eV (two times larger than the default value in VASP, and suitable for these calculations) and 50 k (corresponding to the $9 \times 9 \times 3$ mesh in the Monkhorst-Pack scheme²⁷), respectively. The total energy has converged in each calculation to better than $10^{-4} \text{ eV/(unit cell)}$. The mixing parameter AMIX for the charge density mixing has been considered as 0.8 (VASP default) for YBCO and 0.01 for YSCO, because of the difficulty in convergence of the total energy due to the existence of Sr 5s localized orbital. The number of grid points in the fast Fourier transform mesh, N_{GX} , N_{GY} , and N_{GZ} , have been selected to be 36, 36, and 108 to avoid wrap error. Ion relaxation has been done manually by the change of ionic positions in the force's direction to minimize the ionic forces of the order 1 mRy/ \AA for each pressure. A charge density calculation has been done in $40 \times 40 \times 120$ mesh points in the unit cell. Employing the above criteria, we have calculated the band structure (BS), total density of states (TDOS), electronic charge density (ECD), hole carrier in each plane, equilibrium ionic position, bond lengths, compressibility, and equilibrium unit-cell volume.

RESULTS AND DISCUSSION

The relative z coordination of equilibrium ionic positions of Ba, Sr, Cu(2), O(4), O(3), and O(2) ions at ambient pressure has been derived from ionic relaxation for YBCO and YSCO as 0.18258, 0.35365, 0.15972, 0.3789, 0.3798, and 0.1809, 0.3453, 0.1639, 0.3728, 0.3743, respectively. The data for YBCO at ambient pressure are in good agreement with the experimental study.²⁸ The change of ionic positions by Sr doping (due to p_c) is discussed in the following. The overall shape of BS, TDOS, and ECD and their details for YBCO are in good agreement with accurate calculations by other methods. Comparison of the results with the literature for the YBCO system confirms the capability of the pseudopotential approach by the VASP code for calculation of the electronic structure of mixed HTSC structure, as good as other approaches such as the linear augmented plane-wave (LAPW) or linear muffin-tin orbital (LMTO) methods.²⁹ This does not mean that the pseudopotential VASP code in such calculations has a great advantage over the recent fast

TABLE I. For each pressure, the z equilibrium ionic positions (first line), and their calculated forces (second line) in YBCO.

Pressure/ion	Ba	Cu(2)	O(4)	O(3)	O(2)
-15	0.1842	0.3674	0.1509	0.3837	0.3842
	-0.0033	-0.0059	-0.0116	0.0070	0.0010
-10	0.1838	0.3627	0.1539	0.3822	0.3826
	-0.0014	-0.0116	-0.0258	0.0032	0.0062
-5	0.1829	0.3570	0.1570	0.3805	0.3809
	0.0101	0.0148	-0.0072	0.0038	0.0090
0	0.18258	0.35365	0.15972	0.3789	0.3798
	-0.0021	-0.0048	0.0008	0.0047	-0.0002
5	0.1824	0.3526	0.1616	0.3781	0.3786
	-0.0026	-0.0295	0.0062	-0.0111	-0.0144
10	0.1822	0.3517	0.1635	0.3772	0.3776
	-0.0088	-0.0165	-0.0048	-0.0198	-0.0177
15	0.18188	0.35165	0.1649	0.3762	0.3766
	-0.0086	0.0014	0.0053	-0.0005	-0.0035

full-potential codes such as WIEN2K in regard to both computational and physical points of view; it is just due to our previous experience in its effectiveness in these studies.^{26,30} For YSCO, the general shapes of BS and TDOS are similar to YBCO. The only important difference is the existence of the Sr 5s band near E_F in BS and TDOS, whereas the Ba 6s orbital lies about 10.5 eV below E_F .

To our knowledge of the literature, there is no information about the ionic positions in high pressures (a few GPa) for the systems under study in this work. We have found z , the relative equilibrium ionic positions, for each pressure by a suitable approach: at first, the equilibrium ionic positions in ambient pressure have been used for other pressures, and then the ions were relaxed to their new equilibrium positions. The x and y coordinations have not been changed because of their zero forces due to charge and electronic symmetries, but this does not occur for the z direction. Tables I and II show the z values of the ions and their calculated forces F_z at

their positions for each pressure. It is noted that from the ionic relaxation in this study, and also from the calculated³¹ or experimental³² phonon frequency, one can find that 1 mRy/Å force (considered in this study) can cause the error in the z values of the order 10^{-4} for O(4), Ba, Sr, O(2), and O(3) ions, and 2×10^{-4} for Cu(2) ion. These small uncertainties are out of our discussion in this study and the physics of chemical and mechanical pressures. By the presented forces and phonon frequency information, one can easily obtain the exact equilibrium position ($F_z=0$).

As a first step, we explain the applied mechanical pressure on the ionic positions and the relevance of the expected linear dependence (i.e., constant z values with pressure) of the ionic positions. From Tables I and II, it can be seen that the most important change in the z values is related to z O(4) and z Cu(2) in YBCO with +0.0140 and -0.0158 change, respectively. z Cu(2) in YSCO has a small change with a minimum in 0 to -5 GPa region, and z O(4) in this system has

TABLE II. For each pressure, the z equilibrium ionic positions (first line), and their calculated forces (second line) in YSCO.

Pressure/ion	Sr	Cu(2)	O(4)	O(3)	O(2)
-15	0.1778	0.3472	0.1597	0.3770	0.3779
	-0.0021	0.0085	0.0014	-0.0072	0.0217
-10	0.1804	0.3459	0.16153	0.37498	0.37664
	-0.0613	-0.0154	0.0053	0.0270	0.0023
-5	0.1800	0.3452	0.1629	0.3741	0.3755
	-0.0033	-0.0218	0.0027	-0.0105	-0.0160
0	0.1809	0.3453	0.1639	0.3728	0.3743
	-0.0090	-0.0026	0.0144	-0.0099	-0.0103
5	0.1814	0.3460	0.1651	0.3715	0.3731
	-0.0041	-0.0105	-0.0108	0.0094	0.0165
10	0.1816	0.3473	0.1658	0.37039	0.37227
	0.0042	-0.0074	0.0268	0.0171	0.0110
15	0.1818	0.3488	0.1670	0.36916	0.37071
	0.0097	0.0168	0.0020	0.0148	0.0134

+0.0073, about one-half of the change in YBCO. The change of $zO(2)$ and $zO(3)$ in both compounds is nearly the same with a nearly -0.0075 change. zBa decreases by p_m , while zSr increases, although both changes are small compared to other important changes in these systems. The $zCu(2)$ in YBCO decreases, but this value is nearly constant in the YSCO system. These data indicate an expected linear dependence for Ba, Sr, and Cu(2) for YSCO by p_m , but not for the other atoms, O(4), O(2), and O(3) in both systems, and Cu(2) for YBCO. Determination of the degree of nonlinear dependency in these compounds is important because it causes redistribution of charge density, especially in the CuO_2 planes, which is important in superconducting properties of the layered HTSC's. The largest nonlinear dependency related to the apical oxygen may be due to the stiffness of Cu(1)-O(4) bond relative to the other CuO bonds in these systems. This also affects the positions of the ions in the CuO_2 planes and causes smaller nonlinear dependence for Cu(2), O(2), and O(3). This point will be discussed in the following.

The smaller c lattice parameter and unit-cell volume at ambient pressure, respectively, for YSCO (11.38 Å and 163.90 Å³) relative to YBCO (11.68 Å and 173.57 Å³) are equivalent to the applied pressure of 10 GPa on YBCO.¹⁰ As a result, the YSCO system can be considered as a 10 GPa chemical pressure of YBCO, or YBCO as a -10 GPa (under elongation) of YSCO. Now, we note the contrast between the p_c and p_m dependence of T_c : i.e., $dT_c/dp_c = (dT_c/dx)(dx/dp_c) = (-20) \times 1/10 = -2$ K/GPa [x is the Sr doping in the $Y(Ba_{1-x}Sr_x)_2Cu_3O_{7-\delta}$ compound¹⁰] and $dT_c/dp_m = 0.64$ K/GPa (Ref. 4) for the YBCO system, by considering the z ionic position and the related bond lengths at ambient pressure for both systems. Tables I and II show that p_c has nonlinear dependency for the z values of YBCO except for zBa , i.e., the $zCu(2)$, $zO(4)$, $zO(3)$, and $zO(2)$ are different for YBCO and YSCO. The $zO(4)$ is increased for YSCO, so that the same value for Cu(1)-O(4) bond lengths ($d_{Cu(1)-O(4)} \approx 1.865$ Å) are obtained for both systems. Also, the buckling of the CuO_2 plane, $zO(3)$ and $zO(2)$ - $zCu(2)$ increase by 0.003 for p_c , while for p_m it is nearly constant. The data of $p_m = 10$ GPa for YBCO and ambient pressure for YSCO indicate that p_c has a stronger effect in reducing $zCu(2)$, $zO(3)$, and $zO(2)$ than p_m , while for $zO(4)$, p_m and p_c have the same effect. Similar results can be obtained for the data of -10 GPa of YSCO and YBCO. These results show a linear dependence for zBa and $zO(4)$ on p_c , but this fails for $zCu(2)$, $zO(3)$, and $zO(2)$. So, the contraction of c in YSCO relative to YBCO can result from the large Cu(2)-O(4) contraction. These changes can be considered as the difference between chemical and mechanical pressures in these systems.

Figure 1 shows the change of important bond lengths such as Cu(2)-O(4), Cu(1)-O(4), and CuO_2 -Y- CuO_2 separation versus p_m for YBCO and YSCO. It can be seen that for YBCO the $d_{Cu(1)-O(4)}$ and $d_{Cu(2)-Cu(2)}$ have a maximum at ambient pressure with decreasing negative and positive p_m , while $d_{Cu(2)-O(4)}$ decreases for the whole range. The $d_{Cu(1)-O(4)}$ changes from 1.842 Å for $p = -15$ GPa to 1.859 Å for ambient pressure, and then decreases to 1.839 Å for 15 GPa. This

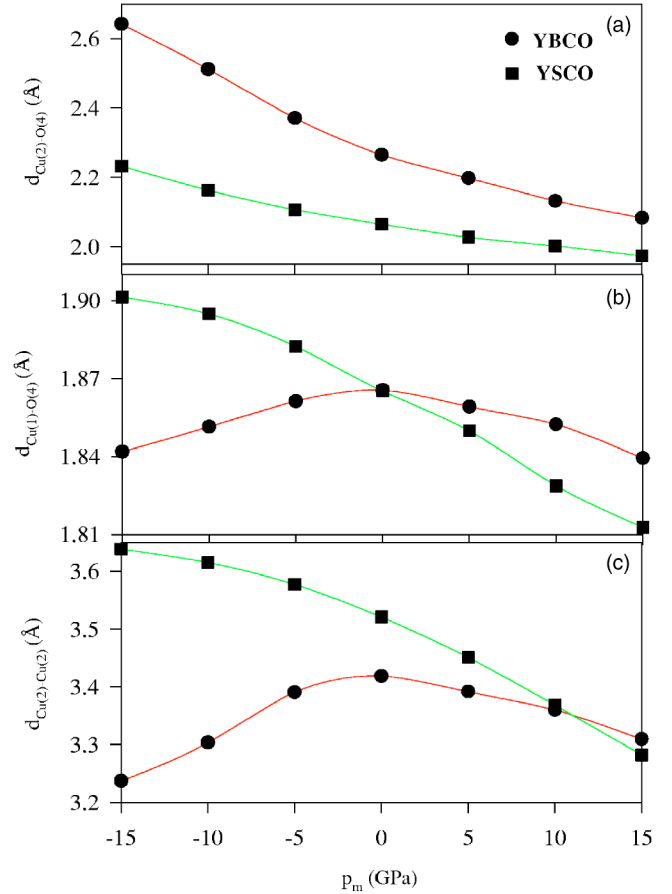


FIG. 1. Distances between Cu(2) and O(4) ions (a), Cu(1) and O(4) ions (b), and between CuO_2 planes (c) for YBCO (circle) and YSCO (square) after ionic relaxation.

small change relative to linear dependence indicates the stiffness of the Cu(1)-O(4) bond, in good agreement with the experimental neutron scattering data.¹⁷ It should be noted that the apical oxygen, the bridge between the superconducting CuO_2 layer and the charge reservoir CuO chain, is important in charge transfer,³³ as will be pointed out in the following. For the positive p_m in YBCO, the change of bond lengths is in the direction of the contraction of c , but for negative p_m , $d_{Cu(1)-O(4)}$ and $d_{Cu(2)-Cu(2)}$ are in the opposite direction of the expansion of c . This shows an attractive force between the CuO chain and O(4), and between the two CuO_2 planes, which is dominated by the expansion of c . This indicates that the system with the large c breaks into two noninteracting subsystems: Cu(1)-O(1)-O(4) and CuO_2 -Y- CuO_2 blocks. Unfortunately, there are no experimental ionic-position data for YBCO under elongation (negative p_m) for comparison and confirmation of this result. It should be noted that although negative mechanical pressure is an interesting physical property, it is hard to produce experimentally. So, we cannot compare our computational data for negative p_m with experiment. Instead, since the reduction of oxygen causes the increase of c lattice parameter,³⁴ the oxygen-deficient $YBa_2Cu_3O_6$ system can be considered as the -5 GPa p_c of $YBa_2Cu_3O_7$. From the neutron studies on this system,³⁵ we see that -5 GPa p_c causes

TABLE III. $10^3 d \ln \chi / dp_m$ for $p_m > 0$ and $p_m < 0$ for YBCO and YSCO and $10^3 d \ln \chi / dp_c$.

$d \ln \chi / dp$	YBCO $p_m > 0$	YBCO $p_m < 0$	YSCO $p_m > 0$	YSCO $p_m < 0$	This calc. p_c	Expt. (Ref. 10) p_c
$\chi = d_{\text{Cu}(2)\text{-O}(4)}$	-5.40	-11.24	-2.89	-5.43	-8.86	-6.08
$\chi = d_{\text{Cu}(1)\text{-O}(4)}$	-0.91	0.87	-1.92	-1.30	0.01	-1.37
$\chi = d_{\text{Cu}(2)\text{-O}(2)}$	-2.10	3.70	-4.54	-2.22	2.99	2.79

the decrease of $d_{\text{Cu}(1)\text{-O}(4)}$ and $d_{\text{Cu}(2)\text{-Cu}(2)}$, in agreement with our result. Because of the importance of charge transfer in the superconductivity of these systems, negative p_m , like the reduction of oxygen content, which divides YBCO into two noninteracting blocks, can result in weakening the superconductivity.

For YSCO, the results are different; all of the bond lengths shown in Fig. 1 decrease by p_m . The $\text{Cu}(1)\text{-O}(4)$ bond length decreases from 1.90 Å to 1.80 Å in YSCO for the whole range of p_m . The change of $d_{\text{Cu}(1)\text{-O}(4)}$ and $d_{\text{Cu}(2)\text{-Cu}(2)}$ in YSCO is larger than that in YBCO, but $d_{\text{Cu}(2)\text{-O}(4)}$ has a smaller change in YSCO. We have calculated $d \ln \chi / dp_m$ with $\chi = d_{\text{Cu}(2)\text{-O}(4)}$, $d_{\text{Cu}(1)\text{-O}(4)}$ and $d_{\text{Cu}(2)\text{-Cu}(2)}$ for $p_m > 0$ and $p_m < 0$ for both systems by a linear fitting of the calculated data in each region. The results are included in Table III. In this table, we have also inserted the $d \ln \chi / dp_c$ calculated by the following Eq. (1) and the experimental data for chemical pressure.¹⁰

$$d \ln \chi / dp_c = (d \ln \chi / dx)(dx / dp_c) \\ = (\chi_{\text{YBCO}} - \chi_{\text{YSCO}}) / \chi_{\text{YBCO}} \times 1/10. \quad (1)$$

Normally, we expect a negative value for $d \ln \chi / dp$, but in Table III there are three positive values that are important to note: two for $p_m < 0$ of YBCO, which is in agreement with the oxygen-deficient system,³⁴ and one for Sr chemical pressure. We note that $d \ln d_{\text{Cu}(2)\text{-Cu}(2)} / dp_c$ has a sign opposite to $d \ln d_{\text{Cu}(2)\text{-Cu}(2)} / dp_m$ for $p_m > 0$ of YBCO, which is an important difference between the p_m and p_c . Increasing of $d_{\text{Cu}(2)\text{-Cu}(2)}$ by 0.1 Å for p_c causes weaker coupling between the CuO_2 planes. It seems that the characteristic structural difference between p_c and p_m has a important role in explaining the opposite change of dT_c / dp_c and dT_c / dp_m in these compounds. A similar conclusion has been obtained by Acha *et al.*¹⁹

The distribution of charge density and their differences by pressure has been plotted in Figs. 2 and 3 for a half-unit-cell of YBCO and YSCO systems, respectively. The distribution of the charge density has been calculated by summation of the 40×40 mesh in each z for all 120 planes perpendicular to the c direction (the $40 \times 40 \times 120$ mesh point has been applied for the charge density calculation). Figures 2(b) and 3(b) show the results at ambient pressure for YBCO and YSCO systems, respectively. The similarity between these figures is due to their similar structural and chemical characteristics. The only considerable difference is the charge density in the SrO layer relative to the BaO layer, due to the absence of the $5p$ orbital in the Sr pseudopotential. The char-

acteristics of these figures have been described in more detail in Ref. 36.

Figures 2(a) and 3(a) and Figs. 2(c) and 3(c) show the difference of the charge distribution of YBCO and YSCO for positive and negative p_m , respectively. This redistribution of the charge density is due to nonlinear contraction or elongation of some bonds in these systems, discussed above. There are three dips and three peaks in the figures for both systems, whose values decrease in the order of the CuO_2 planes, BaO (SrO) planes, and CuO chains. The sign reversal of these dips and peaks by the change in the sign of p_m indicates that these effects are pressure-induced intrinsic effects. The magnitude of the dips and peaks for the negative p_m are larger than those for positive p_m . As can be seen from Fig. 1, bond

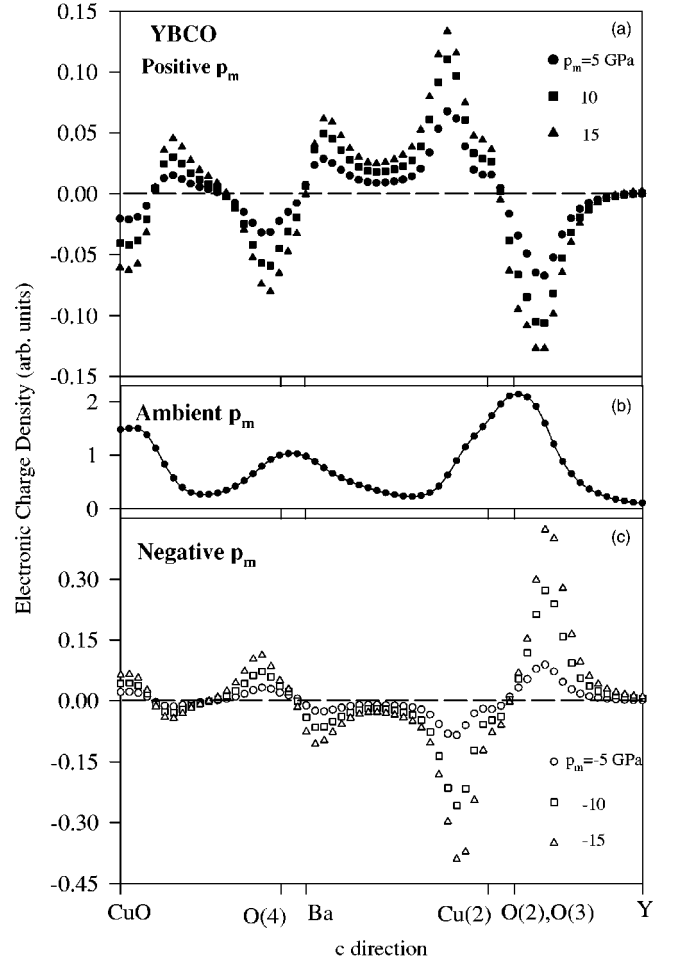


FIG. 2. Total electronic charge density distribution in the c direction for YSCO at ambient pressure (b), and its difference for positive (a) and negative (c) p_m .

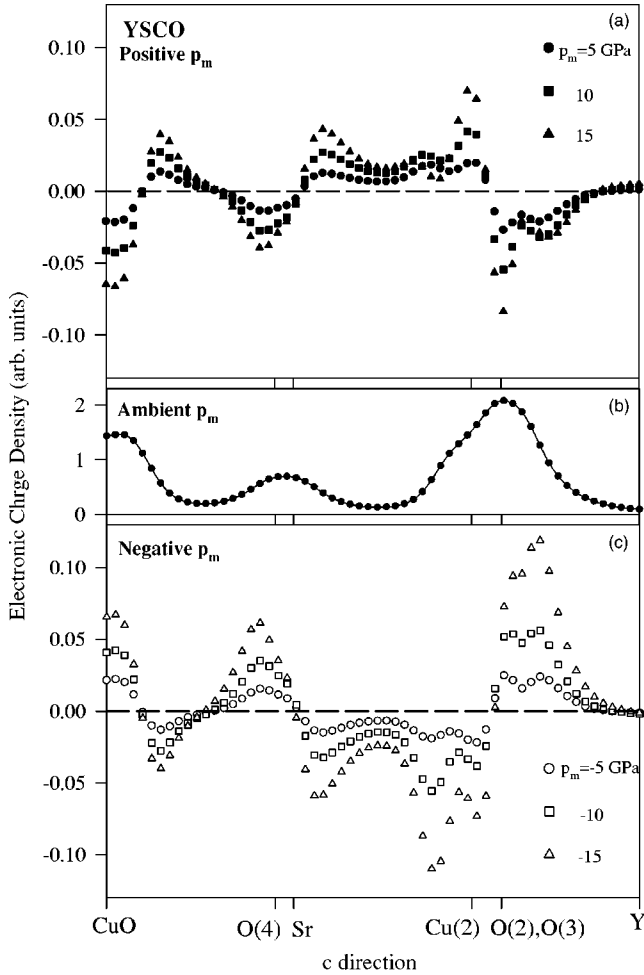


FIG. 3. Total electronic charge density distribution in the c direction for YBCO at ambient pressure (b), and its difference for positive (a) and negative (c) p_m .

lengths have different behavior for the positive and negative p_m , which causes larger charge redistribution for negative p_m relative to positive p_m in both systems. The redistribution of ECD by p_m is higher for YBCO relative to YSCO, which is due to the smaller change of z position in YSCO relative to YBCO. Figures 2 and 3 also show the electric dipole of charge about BaO (SrO) and CuO_2 planes with opposite polarity, although there is no net polarization in the unit cell because of the mirror symmetry to the Y plane. The movement of O(4) upward and movement of Cu(2), O(3), and O(2) downward by p_m have an important role in the electric dipole formation.

The charge redistributions cause charge transfer in the systems. Due to the importance of n_{CuO_2} and n_{CuO} in the superconducting properties of these systems, we have obtained these values by integration of the ECD curve in Figs. 2(b) and 3(b). We have considered the full width at half maximum (FWHM) in each plane as the charge of each layer. The difference of the charge density relative to the ambient pressure for the two systems has been plotted in Fig. 4. As shown in the figure, the electronic charge density has been reduced in both the CuO_2 plane and CuO chain with linear dependence, i.e., both n_{CuO_2} and n_{CuO} increase with p_m .

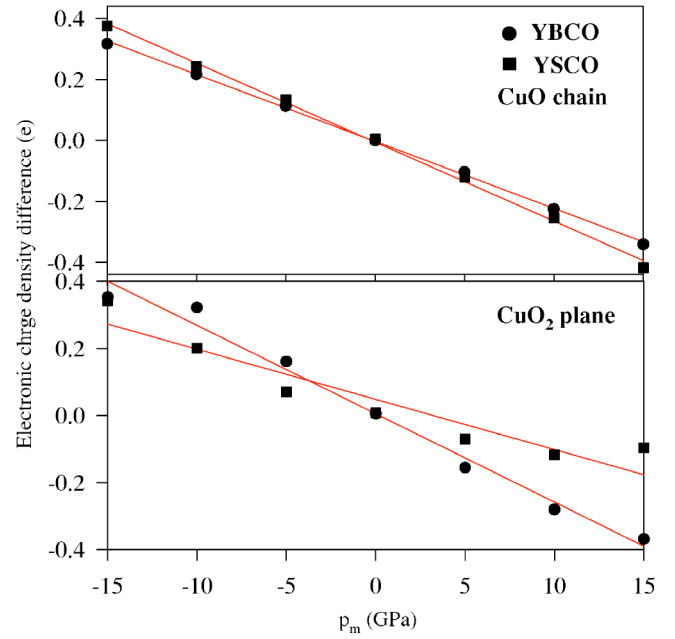


FIG. 4. The change of electronic charge density in the CuO_2 and CuO layers obtained by the FWHM method from the distribution of charge density for YBCO (circle) and YSCO (square) systems. Lines show the linear fit to the data.

This result is in agreement with the experimental reports for the YBCO system.¹⁸ The values of dn_{CuO_2}/dp_m are 0.026 and 0.015 hole/(GPa–unit cell) and of dn_{CuO}/dp_m are 0.022 and 0.026 hole/(GPa–unit cell) for YBCO and YSCO, respectively. The difference between these values and the previous study²⁶ is due to the more accurate calculation and different definition employed for the thickness of the planes (i.e., FWHM) in this study. It should be noted that there is no exact definition for the thickness of the CuO_2 plane, where the change of charge density becomes important there. Other approaches could also be considered in finding the charge transfer to the CuO_2 planes, like the method applied by Ambrosch-Draxl *et al.*³⁷ by considering the change of occupation number of Cu $d_{x^2-y^2}$, O p_x , and O p_y orbitals in the muffin-tin sphere which are included in the full potential LAPW method. But, in this method too the determination of dn_{CuO_2}/dp_m leads to somewhat of an underestimation due to the electronic charge lying inside the muffin-tin sphere (with constant radii in the calculation) while pressure is increased. In the present work the thickness of the layer in terms of the FWHM is about four times larger than the definition in Ref. 26; similar results could be obtained if the same criteria are considered. It seems that there is no hole carrier charge transfer from the CuO reservoir chains to the conducting CuO_2 planes, in agreement with the experimental study.¹⁸

Different values for dn_{CuO_2}/dp_m have been reported in different experiments. From the Hall effect study one can find $dn_{\text{CuO}_2}/dp_m = 0.018$ hole/(GPa–unit cell) ($d \ln n_{\text{CuO}_2}/dp_m = 9\%/\text{GPa}$ with $n_{\text{CuO}_2} = 0.2$),³⁸ but the neutron diffraction study reports $dn_{\text{CuO}_2}/dp_m = 0.0065$ hole/(GPa–unit cell) [$d \ln n_{\text{CuO}_2}/dp_m = (3-4)\%/\text{GPa}$].¹⁷ Comparing the chemical substitution and p_m has resulted in

$dn_{\text{CuO}_2}/dp_m = 0.0055 \text{ hole}/(\text{GPa}\text{-unit cell})$.³⁹ In computational studies, $dn_{\text{CuO}_2}/dp_m = 0.004 \text{ hole}/(\text{GPa}\text{-unit cell})$ (Ref. 40) and $0.0047 \text{ hole}/(\text{GPa}\text{-unit cell})$ (Ref. 41) have been obtained. The value for $\text{HgBa}_2\text{Ca}_{n-1}\text{Cu}_n\text{O}_{2n+2}$ with different n has been obtained to be approximately equal to $0.0033 \text{ hole}/(\text{GPa}\text{-unit cell})$ (Ref. 37), which shows a similar value for different families of HTSC.

We have also fitted the $T_c(p_m)$ data of the YBCO (Ref. 4) and YSCO (Ref. 5) systems by the following equations:^{19,39}

$$\begin{aligned} T_c(n, p_m) &= T_c(n, 0) + \alpha(n)p_m + \beta(n)p_m^2, \\ \alpha(n) &= dT_c^i/dp_m + 2\eta T_c^{\max}(n_{\text{op}} - n)dn/dp_m, \\ \beta(n) &= -\eta T_c^{\max}(dn/dp_m)^2 = -A(dn/dp_m)^2, \\ T_c(n, 0) &= T_c^{\max}[1 - \eta(n_{\text{op}} - n)^2], \end{aligned} \quad (2)$$

where dT_c^i/dp_m is the change of T_c , being independent of charge transfer, T_c^{\max} is the maximum T_c obtained with doping for $p_m=0$, n_{op} is the optimal doping, and η is a constant related to n_{op} . The fitting parameters $T_c(n, 0)$, α , and β have been derived to be 88.96, 1.473, and -0.071 for YBCO and 62.69, 3.796, and -0.438 for YSCO, respectively. We calculated the $dn_{\text{CuO}_2}/dp_m = \frac{1}{2}dn/dp_m = \frac{1}{2}(-\beta/A)^{0.5} = 0.0055 \text{ hole}/(\text{GPa}\text{-unit cell})$ for YBCO and $0.0165 \text{ hole}/(\text{GPa}\text{-unit cell})$ for YSCO. By considering $\eta = \text{const}$ in the two systems, we inserted $A = \eta T_c^{\max} = 590$ (Ref. 15) for YBCO and 416 [$=590 \times 62.69/88.96$; $A^{\text{YSCO}} = A^{\text{YBCO}} T_c^{\text{YSCO}}(n, 0)/T_c^{\text{YBCO}}(n, 0)$] for YSCO. From comparison of the change of T_c by doping and pressure, we find that the value as much as $0.02 \text{ hole}/(\text{GPa}\text{-unit cell})$ is too large for dT_c/dp_m in this system. Thus, we conclude that charge distribution, which participates in the superconducting state are probably confined to a layer with a thickness about 3–4 times smaller than FWHM.

The increase of the calculated n_{CuO_2} by p_m is lower for YSCO than YBCO. To compare our results with experimental reports, we should note that preparation of YSCO (with exact stoichiometry of YBCO) is too hard to achieve. It has been resulted that YSCO forms only under high pressure or substitution of Cu(1) by elements with valence greater than +2.^{5,10} Also, we should note that oxygen content in the family considered here has important effect on the value of dT_c/dp_m , and so it is essential for understanding the pressure effect on T_c . YSCO in high-pressure preparation procedures usually has an oxygen content larger than 7 [i.e., 7.5 (Ref. 5) or 7.2 (Ref. 42)]. Thus, the experimentalists should be aware that the exact quantitative comparison of the calculated parameters in this calculation with experimental data is not our purpose, but the qualitative understanding of the chemical pressure against applied mechanical pressure is followed here. Thus, we compare our results with, for example, the $\text{YSr}_2\text{Cu}_3\text{O}_{7.5}$ sample.⁵ As mentioned by Cao *et al.*,⁵ their $\text{YSr}_2\text{Cu}_3\text{O}_{7.5}$ overdoped samples have $dT_c/dp_m = 3.0 \text{ K/GPa}$, which is in contrast with the PICT model. This is the case since we expect decreasing T_c by applied pressure in the overdoped regime due to the increase of n_{CuO_2} . In spite of the

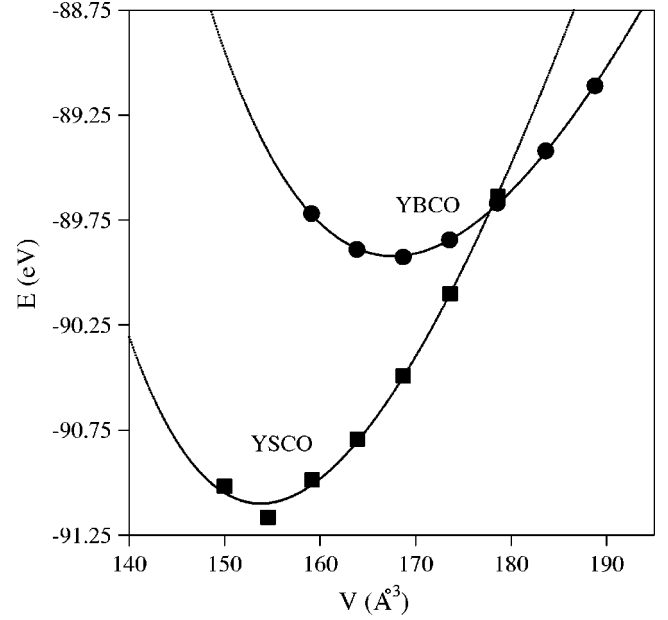


FIG. 5. Total energy of YBCO (circle) and YSCO (square) systems vs their unit-cell volume. The curve shows the fit of data by the Murnaghan equation of state.

lower charge transfer to the CuO_2 plane in YSCO relative to YBCO, the dT_c/dp_m for YSCO is larger than YBCO.

Some reasons are suggested for the above discrepancy: (1) The change of hole content is not the only parameter for determining the dT_c/dp_m , as concluded from other studies.^{19,39} (2) The effect of Sr in superconducting state in this system may be different from Ba in spite of their similar chemical properties; i.e., Ba cations may play an important role in the high- T_c YBCO. (3) The most important effect is probably due to different oxygen content in the $\text{YSr}_2\text{Cu}_3\text{O}_{7.5}$ sample with this calculation, because of the important role of oxygen content in dT_c/dp_m .

To obtain the compressibility and equilibrium volume of both systems, we have fitted the calculated total energy by Murnaghan equation of state.⁴³ In this equation, we have

$$E(V) = E_0 + \{B_0 V [B_{0p}(1 - V_0/V) + (V_0/V)^{B_{0p}} - 1]\} / [B_{0p}(B_{0p} - 1)], \quad (3)$$

where B_0 is the bulk modulus (inverse of compressibility, K_v^{-1}), B_{0p} is the derivation of B_0 at ambient pressure, and V_0 is the equilibrium unit-cell volume. The result of this fitting is plotted for YBCO and YSCO systems in Fig. 5. It can be seen that the calculated data fit very well with Murnaghan's equation of state, which shows the applicability of this equation for the strong anisotropic HTSC materials. The values for B_0 derived from this fitting are 128.3 GPa and 164.2 GPa for YBCO and YSCO systems, respectively. B_0 for YBCO is in good agreement with the calculated value⁴¹ and the experimental result.¹⁷ The larger change of total energy versus volume in YSCO relative to YBCO causes the larger compressibility for YSCO. The value for V_0 has been derived to be 167.67 Å^3 and 153.782 Å^3 for YBCO and YSCO, respectively. These values are lower than the experimental unit-cell

volume (considered in this study) by 3.5% and 6% for YBCO and YSCO systems, respectively. This is not due to the pseudopotential or the details of our calculation, but results from the LDFT approach, as derived also from other studies.^{22,24} From this figure, we see also that the calculated V_0 for YSCO is lower than the value for YBCO, which shows the effect of the chemical pressure. The calculated p_c due to Sr substitution is estimated to be 14 GPa, near the experimental value of 10 GPa.

CONCLUSION

At first, we have shown the capability of pseudopotential VASP code in the calculation of electronic structure of YBCO and YSCO systems. Ionic relaxation calculations indicate a linear dependence for $z\text{Ba}$, $z\text{Sr}$, and $z\text{Cu}(2)$ in YSCO and nonlinear dependence for $z\text{Cu}(2)$ in YBCO, and $z\text{O}(4)$, $z\text{O}(3)$, and $z\text{O}(2)$ in both systems by p_m . The redistribution of charge density by mechanical pressure indicates the transfer of holes to the CuO_2 planes and CuO chains in both systems. The values are derived to be 0.022 and 0.026 hole/(GPa–unit cell) for CuO chains and 0.026 and 0.015 hole/(GPa–unit cell) for the CuO_2 planes, for YBCO and YSCO, respectively. In spite of the larger dT_c/dp_m in YSCO, the

hole content is smaller in YBCO relative to YSCO. The discrepancy between the calculated rate of charge transfer and the experimental studies in both systems has been explained by the role of oxygen content in dT_c/dp_m , and the insufficiency of the PICT model to explain dT_c/dp_m . The chemical pressure causes a nonlinear dependence in YBCO except for $z\text{Ba}$, i.e., the $z\text{Cu}(2)$, $z\text{O}(3)$, and $z\text{O}(2)$ for YBCO are different from the values for YSCO. The $z\text{O}(4)$ is increased for YSCO, so that the same value for Cu(1)–O(4) bond lengths ($d_{\text{Cu}(1)\text{--O}(4)} \approx 1.865 \text{ \AA}$) is obtained for both systems. The increase of $d_{\text{Cu}(2)\text{--Cu}(2)}$ by p_c has an important role in the different dependency of T_c to p_c and p_m . In addition, B_0 has been determined to be 128.3 GPa and 164.2 GPa for YBCO and YSCO, respectively. The smaller calculated $V_0 = 153.78 \text{ \AA}^3$ for YSCO relative to $V_0 = 167.67 \text{ \AA}^3$ for YBCO indicates an effective 14 GPa chemical pressure due to Sr substitution.

ACKNOWLEDGMENTS

The authors wish to thank G. Kresse and J. Furthmüller, the writers of the VASP code. This work was supported in part by the Offices of the Vice President for Research and Dean of Graduate Studies at Sharif University of Technology.

*Author to whom correspondence should be addressed. Electronic address: akhavan@sharif.edu

¹See, for example, C.M. Brown, T. Takenobu, K. Kordatos, K. Prassides, Y. Iwasa, and K. Tanigaki, Phys. Rev. B **59**, 4439 (1999).

²See, for example, R. Kondo, S. Kagoshima, and M. Maesato, Synth. Met. **133–134**, 137 (2003).

³J.S. Schilling and S. Klotz, in *Physical Properties of High Temperature Superconductors III*, edited by D.M. Ginsberg (World Scientific, Singapore, 1992), pp. 59–157.

⁴S.W. Tozer, J.L. Koston, and E.M. McCarron III, Phys. Rev. B **47**, 8089 (1993).

⁵Y. Cao, T.L. Hudson, Y.S. Wang, S.H. Xu, Y.Y. Xue, and C.W. Chu, Phys. Rev. B **58**, 11 201 (1998).

⁶B. Bucher, J. Karpinski, E. Kaldis, and P. Wachter, Physica C **157**, 478 (1989).

⁷J. Ye, Z. Zou, A. Matsushita, K. Oka, Y. Nishihara, and T. Matsumoto, Phys. Rev. B **58**, R619 (1998).

⁸R. Benischke, T. Weber, W.H. Fietz, J. Metzger, K. Grube, T. Wolf, and H. Wuhl, Physica C **203**, 293 (1992).

⁹G. Baskaran, Phys. Rev. Lett. **90**, 197007 (2003).

¹⁰F. Licci, A. Gauzzi, M. Marezio, G.P. Radaelli, R. Masini, and C. Chaillout-Bougerol, Phys. Rev. B **58**, 15 208 (1998).

¹¹A.A.R. Fernandes, J. Santamaria, S.L. Bud'ko, O. Nakamura, J. Guimpel, and I.K. Schuller, Phys. Rev. B **44**, 7601 (1991).

¹²T.R. Lu and T.M. Chen, Physica C **276**, 75 (1997).

¹³R.S. Liu, J.S. Ho, C.T. Chang, and P.P. Edwards, J. Solid State Chem. **92**, 247 (1991).

¹⁴Y. Itoh, S. Adachi, T. Machi, and N. Koshizuka, Phys. Rev. B **64**, 180511(R) (2001).

¹⁵B.K. Agrawal and S. Agrawal, Phys. Rev. B **52**, 12 556 (1995).

¹⁶E.V.L. de Mello and C. Acha, Phys. Rev. B **56**, 466 (1997).

¹⁷J.D. Jorgensen, S. Pei, P. Lightfoot, D.G. Hinks, B.W. Veal, B. Dabrowski, A.P. Paulikas, and R. Kleb, Physica C **171**, 93 (1990).

¹⁸K. Yoshida, A.I. Rykov, S. Tajima, and I. Terasaki, Phys. Rev. B **60**, R15 035 (1999).

¹⁹C. Acha, M. Nunez-Regueiro, S. Le Floch, P. Bordet, J.J. Capponi, C. Chaillout, and J.-L. Tholence, Phys. Rev. B **57**, R5630 (1998).

²⁰C. Ambrosch-Draxl, R. Abt, and P. Knoll, Physica C **235–240**, 2119 (1994); C. Ambrosch-Draxl, R. Kouba, and P. Knoll, Z. Phys. B: Condens. Matter **104**, 687 (1997).

²¹M. Cardona, Physica C **317–318**, 30 (1999).

²²R. Kouba, C. Ambrosch-Draxl, and B. Zangger, Phys. Rev. B **60**, 9321 (1999).

²³H. Kim and J. Ihm, Phys. Rev. B **51**, 3886 (1995).

²⁴T. Thonhauser, H. Auer, E.Ya. Sherman, and C. Ambrosch-Draxl, Phys. Rev. B **69**, 104508 (2004).

²⁵G. Kresse and J. Furthmüller, Comput. Mater. Sci. **6**, 15 (1996); Phys. Rev. B **54**, 11 169 (1996).

²⁶H. Khosroabadi, M.R. Mohammadzadeh, and M. Akhavan, Physica C **370**, 85 (2002).

²⁷H.J. Monkhorst and J.D. Pack, Phys. Rev. B **13**, 5188 (1976).

²⁸R.M. Hazen, in *Physical Properties of High Temperature Superconductors II*, edited by D.M. Ginsberg (World Scientific, Singapore, 1998), Chap. 3.

²⁹W.E. Pickett, Rev. Mod. Phys. **61**, 433 (1989).

³⁰H. Khosroabadi, B. Mossalla, and M. Akhavan, Phys. Status Solidi C **1**, 1867 (2004).

³¹R.E. Cohen, W.E. Pickett, and H. Krakauer, Phys. Rev. Lett. **64**, 2575 (1990).

- ³²K.F. McCarty, J.Z. Liu, R.N. Shelton, and H.B. Radousky, *Phys. Rev. B* **41**, 8792 (1990).
- ³³H. Khosroabadi and M. Akhavan, *Phys. Status Solidi C* **1**, 1871 (2004); L.F. Feiner, M. Grilli, and C. deCastro, *Phys. Rev. B* **45**, 10 647 (1992).
- ³⁴R.J. Cava, A.W. Hewat, E.A. Hewat, B. Batlogg, M. Marezio, K.M. Rabe, J.J. Krajewski, W.F. Peck, Jr., and L.W. Rupp, Jr., *Physica C* **165**, 419 (1990).
- ³⁵J.D. Jorgensen, B.W. Veal, A.P. Paulikas, L.J. Nowicki, G.W. Crabtree, H. Claus, and W.K. Kwok, *Phys. Rev. B* **41**, 1863 (1990).
- ³⁶H. Khosroabadi, M.R. Mohammadizadeh, and M. Akhavan, *Physica B* **321**, 360 (2002).
- ³⁷C. Ambrosch-Draxl, E.Ya. Sherman, and H. Auer, *Phys. Rev. Lett.* **92**, 187004 (2004).
- ³⁸C. Murayama, Y. Iye, T. Enomoto, A. Fukushima, N. Mori, Y. Yamada, and T. Matsumoto, *Physica C* **185–189**, 40 (1991).
- ³⁹J.J. Neumeier and H.A. Zimmermann, *Phys. Rev. B* **47**, 8385 (1993).
- ⁴⁰R.P. Gupta, and M. Gupta, *Phys. Rev. B* **50**, 9615 (1994).
- ⁴¹X.J. Chen, C.D. Gong, and Y.B. Yu, *Phys. Rev. B* **61**, 3691 (2000).
- ⁴²O.I. Lebedev, G. Van Tendeloo, F. Licci, E. Gilioli, A. Gauzzi, A. Prodi, and M. Marezio, *Phys. Rev. B* **66**, 132510 (2002).
- ⁴³D. Murnaghan, *Proc. Natl. Acad. Sci. U.S.A.* **30**, 244 (1944).